Available online at www.sciencedirect.com

SciVerse ScienceDirect

Ceramics International 39 (2013) 1209–1214

CERAMICS INTERNATIONAL

www.elsevier.com/locate/ceramint

High erosion resistant Y_2O_3–carbon electroconductive composite under the fluorocarbon plasma

Kwan-Young Choi, Yoon-Suk Oh, Seongwon Kim, Sung-Min Lee*

Engineering Ceramic Center, Korea Institute of Ceramic Engineering and Technology (KICET), Icheon-si, Gyeonggi-do 467-843, Republic of Korea

Received 15 June 2012; received in revised form 18 June 2012; accepted 16 July 2012
Available online 23 July 2012

Abstract

A new plasma-resistant composite with electrical conductance has been developed for use in the plasma processing equipments of the semiconductor industry. Currently, electrical conductive silicon is widely used as parts for the wafer processing equipments, but its erosion rate is too fast, causing short life time of the parts. In this study, yttrium oxide, which has a high erosion resistance under fluorocarbon plasmas, was used as a matrix material and carbon was added for a conducting phase. The threshold fraction of carbon for the conductance depended on the carbon sources as well as the sintering temperature. The current flow through the carbon phases inside the composite was demonstrated through a scanning probe microscopy technique. The developed composite has an electrical conductivity around 0.01 S/cm with a threshold carbon of 0.6 wt%, at a density of more than 99%; its plasma resistance was about 15 times greater than that of silicon. The developed composite can be used as a substitute for the electrically conductive silicon parts in wafer processing equipments.

Keywords: Composite; Electrical conductance; Plasma erosion resistance; Yttrium oxide

1. Introduction

The semiconductor industry uses many materials for the plasma-facing parts of wafer processing equipments [1–8]. Such materials include silicon, silicon dioxide, sintered Al_2O_3 or Y_2O_3, and Y_2O_3 coatings. The choice of material depends on the application position inside the processing chamber, and the selection criteria include plasma resistance, electrical properties, and the possibility of producing contamination particles.

By plasma discharge, the fluorocarbon gases decompose to reactive radicals and ions, which react with the surface of parts to form etch products, which are successively removed by sputtering or evaporation [4,5,9–11]. For instance, silicon fluoride, which is formed by the interaction between fluorocarbon plasma and silicon, has a high vapor pressure, so it evaporates easily causing a fast erosion of the silicon [9–12]. Even though silicon has low plasma erosion resistance, it has been widely used as plasma-facing parts in the industry because it has electrical conductivity, similar to that of silicon wafers. It has been applied to the cathode so that it can deliver electrical power to sustain the plasma inside the chamber. Also, if silicon is used as focus rings, it can provide better plasma uniformity over silicon wafer due to its similar electrical conductivity with the wafer. As stated above, silicon is a very useful material in the parts applications, but its high erosion rate under the fluorocarbon plasma severely shortens life time and significantly increases the cost of wafer processing.

In this study, we tried to develop a new material with a high plasma resistance thus longer life time as well as electrical conductance. Kim et al. [4] showed that oxide ceramics such as aluminum/yttrium oxide have a superior erosion resistance under fluorocarbon plasma. Yttrium oxide, in particular, has the lowest etch rate and, consequently, the highest level of plasma resistance. We fabricated a composite of yttrium oxide and an electrically conducting phase. We selected carbon for the conducting phase because it is one of the elements of usual fluorocarbon plasma and

*Corresponding author. Tel.: +82 31 645 1441; fax: +82 31 645 1492.
E-mail address: smlee@kicet.re.kr (S.-M. Lee).

0272-8842/$ - see front matter © 2012 Elsevier Ltd and Techna Group S.r.l. All rights reserved.
http://dx.doi.org/10.1016/j.ceramint.2012.07.046

can be used safely in wafer processing. If the carbon acts as a current path, then, according to the literatures on percolation thresholds [13–15], the threshold volume fraction of carbon for the conductance may depend on the size ratio of the matrix to the conducting phase. In this study, different sources of carbon were tested: micrometer-sized carbon, nano-sized carbon, and carbons from phenol resin. We measured the electrical conductivity in relation to the carbon sources, amount of carbon and sintering temperature. The microstructure was analyzed by means of scanning electron microscopy (SEM) and transmission electron microscopy (TEM). To confirm the current flow through the dispersed carbons, we used a scanning probe microscopy technique.

2. Experimental procedures

We selected Y_2O_3 powder (0.3 μm, C-grade, H.C. Starck, 15 m^2/g, Germany) as a matrix material. For the conducting phase, we used fine micrometer-sized carbon (8.5 m^2/g, Seunglim Carbon Co, Korea) or nano-sized carbon (35.4 m^2/g, N774, Orion Evonic Co., USA); we also tested phenol resin (CB-8060 K, Kangnam Chemical Co., Korea) as a carbon source. When the phenol resin was heat-treated at 800 °C, its initial weight was reduced by around 70%; that was considered to make a mixed powder with the specified nominal carbon content. The Y_2O_3 powder was mixed with the carbon sources by using ball milling in ethanol media with Al_2O_3 balls for 20 h. The prepared powders were dried on a hot plate and in an oven at 80 °C for 12 h and then softly pulverized. The mixed powder was sintered using a hot-press technique at two different temperatures of 1400 °C or 1600 °C for 1 h, under a pressure of 20 MPa and a nitrogen atmosphere. We used a graphite mold and punches for hot-pressing of the powders. When the phenol resin was added, the powder was heat-treated at 800 °C for 1 h during the sintering process to convert the phenol resin to a carbon phase.

The electrical conductivity of the sintered body was measured by means of a two-probe method after platinum electrodes were deposited on both sides of the specimen. The crystalline structure of the sintered composite was analyzed with an X-ray diffractometer (D/max-2500, Rigaku, Japan) on the crushed powder of the sintered body. For the microstructure analysis, the specimens were polished with diamond pastes to 1 μm surface finish. The polished surface was then observed with a scanning electron microscope (JSM-6071F, Jeol, Japan) to obtain back-scattered electron images, which show a clear contrast between the carbon phase and the yttrium oxide matrix phase. The specimen was thinned with a focused ion beam (Helios 600, FEI Co., USA) and observed with a transmission electron microscope (Tecnai F30, FEI, Netherlands).

To confirm the conducting mechanism, we used a scanning probe microscope (XE-150, Park System, Korea). While a bias voltage of 5 V was applied to the specimen, the polished surface was probed with a conductive cantilever coated with platinum. A surface area of 100×100 μm^2 was probed, and the current flow through the conductive cantilever was monitored. The plasma resistance of the composite was measured with an inductively coupled plasma etcher (NIE 150, NTM Co, Korea) which used CF_4, O_2, and Ar as processing gases. Table 1 shows the details of the etch conditions.

Table 1
Details of plasma etch conditions.

Parameters	Condition
RF power (W)	600
RF bias voltage (V)	450
Pressure (mTorr)	10
CF_4:O_2:Ar (SCCM)	30:5:10
Etch time (min)	120

3. Results and discussion

Fig. 1 shows the densification behavior of the yttrium oxide–carbon composite in relation to the various sources of carbon. The densification was retarded when a higher amount of nano-sized carbon was used at a sintering temperature of 1400 °C. As the sintering temperature increased to 1600 °C, the densification of the composites exceeded 98% and there was less dependence on the carbon content. The densification behavior was similar when the phenol resin was used as a carbon source, though the density was slightly lower at a sintering temperature of 1400 °C than when the nano-carbon was added. In contrast with other carbon sources such as nano-sized carbon or phenol resin, the micrometer-sized carbon has no great effect on densification. Even the addition of 5 wt% of carbon leads to a minor inhibition of the densification process.

The yttrium oxide remained intact during sintering, producing no oxycarbide or carbide phases (Fig. 2). A few literatures [16,17] suggest that yttrium oxycarbide may form from the reaction between carbon and yttrium oxide with a weight loss due to the emission of CO gas. However, in our experiment, we could not see any trace of the oxycarbide phase, which seems to be due to the suppression of gas evolution from a relatively fast densification by hot-pressing. Therefore, the yttrium oxide and the added carbon were well densified to a composite.

Fig. 3 shows the microstructure of an Y_2O_3–carbon composite and its electrical conductivity when micrometer-sized carbon was used. The microstructure consisted of an Y_2O_3 matrix and aligned plate-like carbons. The carbon plates, which have a length of around 10 μm with a thickness of around 1 μm, were aligned in a direction perpendicular to the hot-pressing. Thus, the structure seems to be a result of the composite's one-dimensional shrinkage, which was induced by the hot-pressing technique. Fig. 3(b) shows that the composites were insulating upto 5 wt% of the added micrometer-sized carbon,

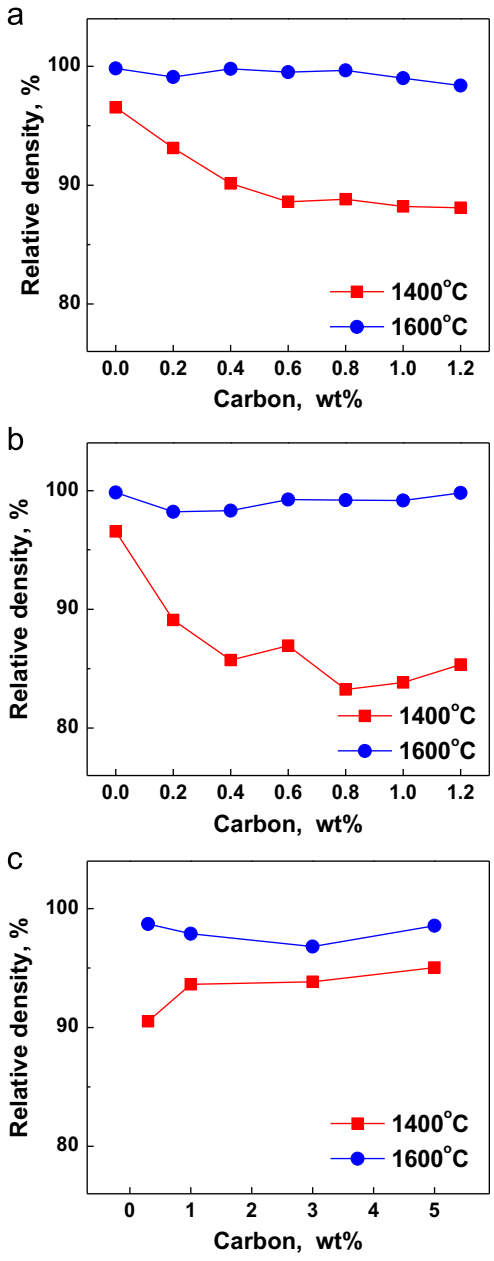

Fig. 1. Electrical conductivities of Y_2O_3–carbon composites sintered at 1400 °C or 1600 °C for 1 h using different sources of carbon: (a) nano-carbon, (b) phenol resin and (c) micrometer-sized carbon.

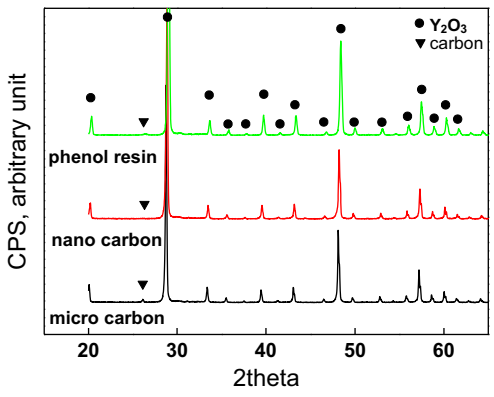

Fig. 2. X-ray diffraction patterns of Y_2O_3–carbon composites sintered at 1600 °C using different sources of carbon.

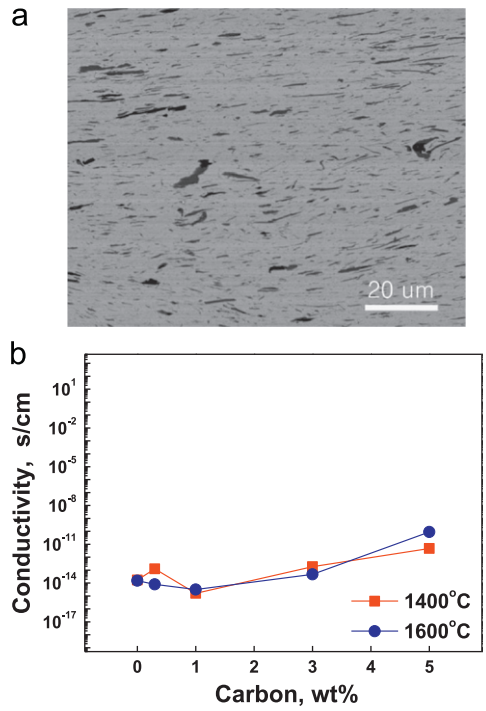

Fig. 3. (a) Microstructure of a composite with micrometer-sized carbon of 5 wt% sintered at 1600 °C and (b) electrical conductivities with various amounts of the carbon.

regardless of the sintering temperature. When the added carbon exceeded 3 wt%, the conductivity was slightly increased, but the increase was marginal and insufficient to provide an adequate electrical conductivity to the sintered composites.

The use of nano-sized carbon or phenol resin as a carbon source was a very effective in making the conductive composites (Fig. 4). When nano-carbon was added, the composite sintered at 1400 °C was electrically conductive even at 0.2 wt% addition. As the sintering temperature increased to 1600 °C, the percolation threshold for the electrical conductivity increased to 0.6 wt%. The sintered body with more than 0.6 wt% of carbon has a conductivity level around 10^{-2} S/cm, which is similar to that of silicon used in the semiconductor industry. When the phenol resin was used, the specimens sintered at 1400 °C showed electrical conductivity similar to those of the nano-carbon composites (Fig. 4(b)). However, at higher sintering temperatures, they transformed to insulating materials in the studied range of carbon.

Fig. 5 shows the microstructures of sintered bodies that use nano-sized carbon or phenol resin as a carbon source with a nominal amount of 1 wt% carbon. The microstructure contained very thin plate-like carbons, which were dispersed uniformly throughout the specimen. Though the carbon phases in both specimens look isolated, the specimen with nano-carbon is conductive, whereas the specimen with

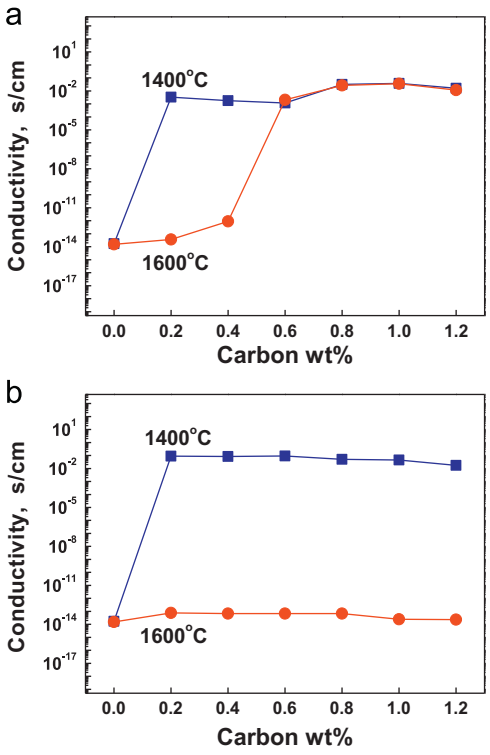

Fig. 4. Electrical conductivities of Y_2O_3–carbon composites sintered at 1400 °C or 1600 °C using two different sources of carbon: (a) nano-sized carbon and (b) phenol resin.

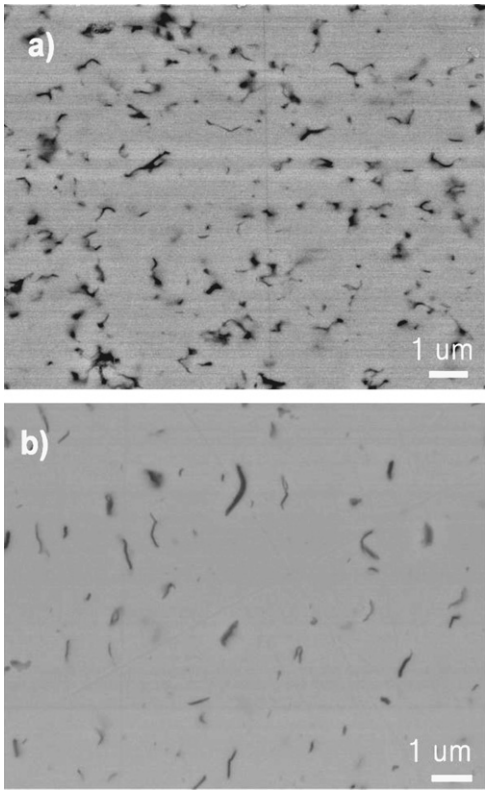

Fig. 5. Microstructures of Y_2O_3–carbon composites with nominal 1 wt% of carbon sintered at 1600 °C using two different sources of carbon: (a) nano-sized carbon and (b) phenol resin.

carbon from phenol resin is insulating as shown in Fig. 4. This difference in the effect of nano-carbon or phenol resin on the electrical conductivity for the same nominal amount of carbon phases may be explained in terms of difference in the actual carbon content. As shown in Fig. 5, the amount of carbon in the specimen from the phenol resin seems to be less than the amount of carbon in the specimen that uses nano-carbon. Actually, the measured carbon contents were 1.3% for the composite with nano-sized carbon and 0.6% for the composite from phenol resin for the same nominal 1 wt% of carbon. We have added an extra amount of phenol resin to get the same nominal amount of carbon, based on the conversion ratio of the phenol resin measured at 800 °C. However, the phenol resin may possibly undergo more weight loss at a higher sintering temperature, resulting in reduced carbon content.

From the transmission electron microscopy, we could easily identify the carbon phase by comparing high angle annular dark field (HAADF) and bright field images, because carbon phase was dark in the HAADF image. The microstructure of the specimen sintered at 1600 °C with 1 wt% of nano-sized carbon has two kinds of carbon morphology: a thin plate-like morphology or an agglomerated morphology. The thin plate-like carbon phases were as thin as 20 nm; they have a crystalline structure (Fig. 6(a)). In contrast, the carbons, which are slightly agglomerated in the Y_2O_3 grain junction, were mostly amorphous. Besides the carbon phases, we could not see any impurity-related phases.

The percolation threshold, about 0.6 wt%, for electrical conductance corresponds to approximately 1.5 vol% considering the density difference between carbon and yttrium oxide. If 1.5 vol% was the case for spherical conducting phase as in a model based on the segregated network [18], the size ratio of the matrix and conducting phases must be far larger than 35. However, actual apparent carbon size was not so small, considering its specific surface area 35.4 m^2/g, compared to 15.0 m^2/g for Y_2O_3. So, this low threshold cannot be attributed to the size ratio, but to the shape of conducting phase. As shown in Figs. 5 and 6, carbons were mostly very thin and plate-like. This thin plate shape must have significant effects on constructing a network for electrical conductance. In these regards, the effect of sintering time might be considered. At higher sintering temperature, grain growth of the matrix phase may result in the coalescence of carbon phase with loss of electrical conductance of the composite.

A current flow map was obtained from the application of scanning probe microscopy to the specimen with 1 wt% nano-sized carbon sintered at 1600 °C. Fig. 7 shows the current map of a 100 × 100 μm^2 area of the polished surface. The black indicates a high current flow area and the white part indicates the insulating area. The map showed that the current flowed discretely at points on the surface, not uniformly through the matrix, confirming the electrical conductance through the dispersed carbon phases. It is also noted that the average distance between the current flowing spots was around a few micrometers, several times longer than the inter-carbon distance observed in Fig. 5(a), implying

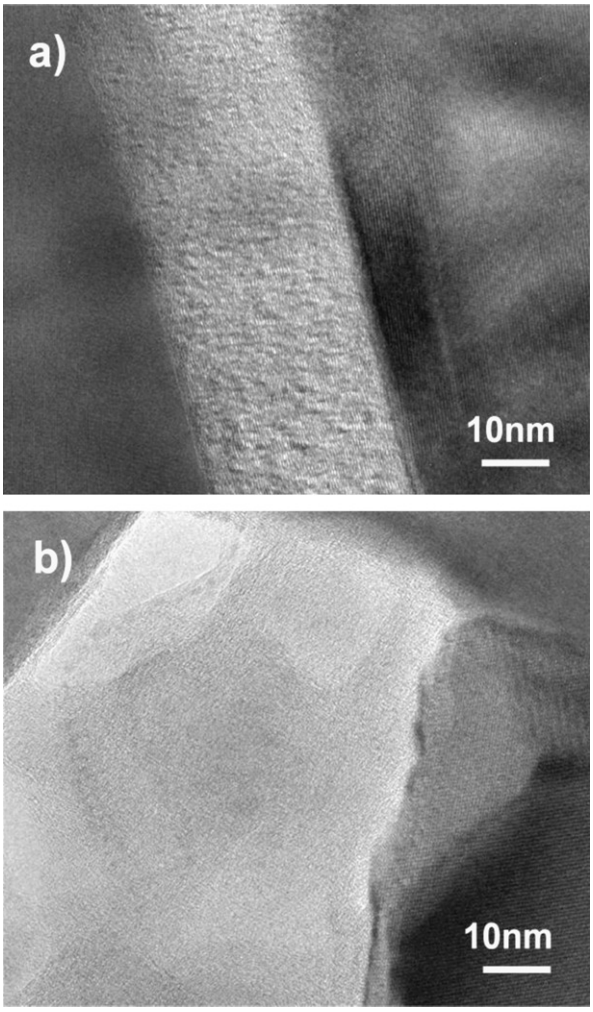

Fig. 6. TEM microscopies of two different carbon morphologies observed in the composite with 1 wt% of nano-carbon sintered at 1600 °C: (a) crystalline plate-like and (b) amorphous agglomerated carbon.

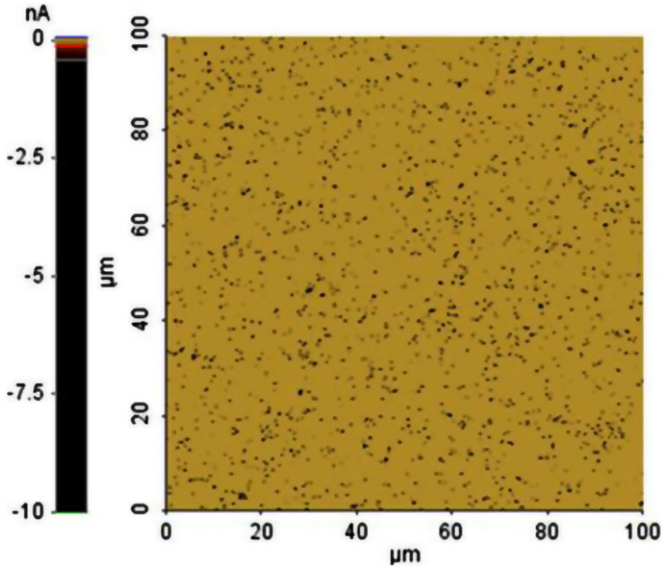

Fig. 7. Current flow map of the specimen with 1 wt% nano-carbon sintered at 1600 °C from scanning probe microscopy using a conductive cantilever.

that only some portion of the carbon contributed to the conductance.

The plasma resistance of the composite with 1 wt% nano-carbon sintered at 1600 °C was superior to that of the silicon reference material, though it has similar electrical conductivity with that of silicon. Fig. 8 shows the cross-sections of the etched composite and silicon reference material. On account of the high plasma resistance of the Y_2O_3 matrix, the etch rate of the conductive composite was 15 times lower than that of silicon. So the developed composite has high plasma resistance as well as an electrical conductance. As a result, it may be a new candidate material for the various silicon parts, such as electrodes and focus rings in plasma processing equipments, providing much longer life time of the parts made of the composite.

4. Conclusion

An electrically conductive composite with a high level of plasma resistance was developed. The composite consisted

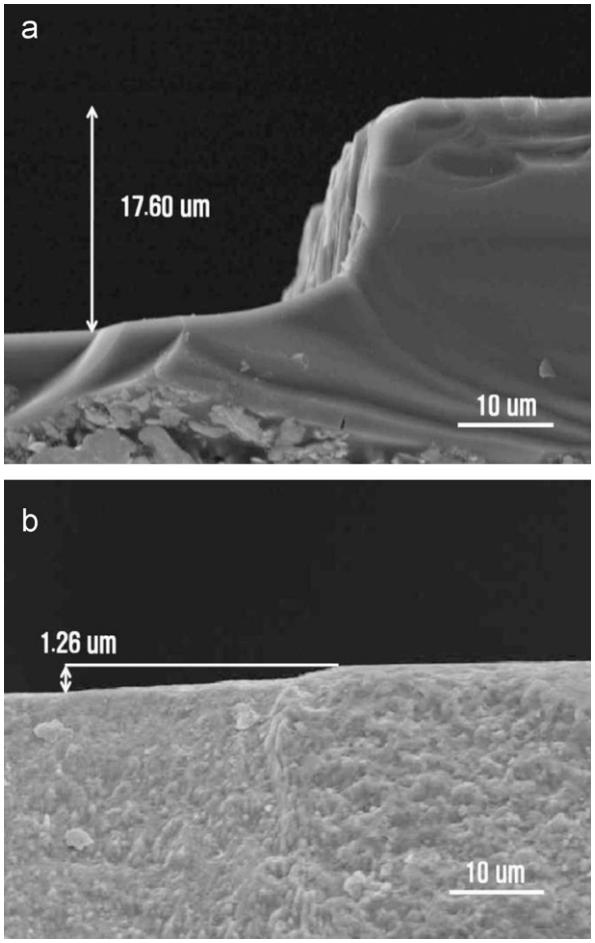

Fig. 8. Cross-sectional images of plasma etched specimen using Ar, CF_4 and O_2 as reaction gases: (a) silicon and (b) composite with 1 wt% nano-carbon sintered at 1600 °C.

of a plasma resistant Y_2O_3 matrix and electrically conductive carbon. The threshold fraction of carbon for electrical conductance depends on the source of the carbon and the sintering temperature. Nano-sized carbon, which is more effective than micrometer-sized carbon, has a threshold fraction of 0.6 wt% for the electrical conductance of the dense composite when the composite was sintered at 1600 °C. Through the scanning probe microscopy technique, we confirmed that the current flowed discretely at points on the surface rather than through the matrix. This low percolation threshold for the conductance may be explained in terms of the shape of the conducting phase. The fact that etch rate of the developed composite under typical plasma is 15 times lower than that of silicon indicates that the composite may be used as a substitute for silicon parts in plasma processing equipments.

References

[1] Y. Kobayashi, Current Status and Needs in the Future of Ceramics Used for Semiconductor Production Equipment, Osaka, Japan, July, 2005, The 37th Seminar on High Temperature Ceramics, 2005, pp. 17.

[2] N. Ito, T. Moriya, F. Uesugi, M. Matsumoto, S. Liu, Y. Kitayama, Reduction of particle contamination in plasma-etching equipment by dehydration of chamber wall, Japanese Journal of Applied Physics 47 (2008) 3630–3634.

[3] M. Schaepkens, R.C.M. Bosch, T.E.F.M. Standaert, G.S. Oehrlein, J.M. Cook, Influence of reactor wall conditions on etch processes in inductively coupled fluorocarbon plasmas, Journal of Vacuum Science and Technology A 16 (1998) 2099–2107.

[4] D.M. Kim, S.H. Lee, W.B. Alexander, K.B. Kim, Y.S. Oh, S.M. Lee, X-ray photoelectron spectroscopy study on the interaction of yttrium–aluminum oxide with fluorine-based plasma, Journal of the American Ceramic Society 94 (2011) 3455–3459.

[5] D.M. Kim, Y.S. Oh, S.W. Kim, H.T. Kim, D.S. Lim, S.M. Lee, The erosion behaviors of Y_2O_3 and YF_3 coatings under fluorocarbon plasma, Thin Solid Films 519 (2011) 6698–6702.

[6] D.M. Kim, K.B. Kim, S.Y. Yoon, Y.S. Oh, H.T. Kim, S.M. Lee, Effects of artificial pores and purity on the erosion behaviors of polycrystalline Al_2O_3 ceramics under fluorine plasma, Journal of the Ceramic Society of Japan 117 (2009) 863–867.

[7] K.B. Kim, D.M. Kim, J.G. Lee, Y.S. Oh, H.T. Kim, H.S. Kim, S.M. Lee, Erosion behavior of YAG ceramics under fluorine plasma and their XPS analysis, Journal of the Korean Ceramic Society 46 (2009) 456–461.

[8] J. Iwasawa, R. Nishimizu, M. Tokita, M. Kiyohara, K. Uematsu, Plasma resistant dense yttrium oxide film prepared by aerosol deposition process, Journal of the American Ceramic Society 90 (2007) 2327–2332.

[9] T.E.F.M. Standaert, M. Schaepkens, N.R. Rueger, P.G.M. Sebel, G.S. Oehrlein, J.M. Cook, High density fluorocarbon etching of silicon in an inductively coupled plasma: mechanism of etching through a thick steady state fluorocarbon layer, Journal of Vacuum Science and Technology A 16 (1998) 239–249.

[10] T.E.F.M. Standaert, C. Hedlund, E.A. Joseph, G.S. Oehrlein, T.J. Dalton, Role of fluorocarbon film formation in the etching of silicon, silicon dioxide, silicon nitride, and amorphous hydrogenated silicon carbide, Journal of Vacuum Science and Technology A 22 (2004) 53–60.

[11] M. Matsui, T. Tatsumi, M. Sekine, Observation of surface reaction layers formed in highly selective SiO_2 etching, Journal of Vacuum Science and Technology A 19 (2001) 1282–1288.

[12] K. Kurihara, Y. Yamaoka, K. Karahashi, M. Sekine, Measurements of desorbed products by plasma beam irradiation on SiO_2, American Vacuum Society A 22 (2004) 2311–2314.

[13] Da He, N.N. Ekere, Effect of particle size ratio on the conducting percolation threshold of granular conductive-insulating composites, Journal of Physics D: Applied Physics 37 (2004) 1848–1852.

[14] A. Malliaris, D. Turner, Influence of particle size on the electrical resistivity of compacted mixtures of polymeric and metallic powders, Journal of Applied Physics 42 (1971) 614–618.

[15] R.P. Kusy, Influence of particle size ratio on the continuity of aggregates, Journal of Applied Physics 48 (1977) 5301–5305.

[16] C.E. Holcombe, D.A. Carpenter, Identification of a new yttrium oxycarbide, Y_2OC, Journal of the American Ceramic Society 64 (1981) 82–83.

[17] V. Brozek, P. Karen, B. Hajek, Studies of hydrolysable carbides XXVI: composition limits of the NaCl-type yttrium oxycarbide phase, Journal of the Less Common Metals 107 (1985) 295–299.

[18] W.J. Kim, M. Taya, K. Yamada, N. Kamiya, Percolation study on electrical resistivity of SiC/Si_3N_4 composites with segregated distribution, Journal of Applied Physics 83 (1988) 2593–2598.